COMPEL - The international journal for computation and mathematics in electrical and electronic engineering

Effect of mechanical stress on different iron loss components up to high frequencies and magnetic flux densities

Jan Karthaus, Simon Steentjes, Nora Leuning, Kay Hameyer,

Received 19 September 2016
Revised 26 January 2017
Accepted 31 January 2017

Effect of mechanical stress on different iron loss components up to high frequencies and magnetic flux densities

Jan Karthaus, Simon Steentjes, Nora Leuning and Kay Hameyer
Institute of Electrical Machines,
Rheinisch Westfälische Technische Hochschule Aachen, Aachen, Germany

Abstract

Purpose – The purpose of this paper is to study the variation of the specific iron loss components of electrical steel sheets when applying a tensile mechanical load below the yield strength of the material. The results provide an insight into the iron loss behaviour of the laminated core of electrical machines which are exposed to mechanical stresses of diverse origins.

Design/methodology/approach – The specific iron losses of electrical steel sheets are measured using a standardised single-sheet tester equipped with a hydraulic pressure cylinder which enables application of a force to the specimen under test. Based on the measured data and a semi-physical description of specific iron losses, the stress-dependency of the iron loss components can be studied.

Findings – The results show a dependency of iron loss components on the applied mechanical stress. Especially for the non-linear loss component and high frequencies, a large variation is observed, while the excess loss component is not as sensitive to high mechanical stresses. Besides, it is shown that the stress-dependent iron loss prediction approximates the measured specific iron losses in an adequate way.

Originality/value – New applications such as high-speed traction drives in electric vehicles require a suitable design of the electrical machine. These applications require particular attention to the interaction between mechanical influences and magnetic behaviour of the machine. In this regard, knowledge about the relation between mechanical stress and magnetic properties of soft magnetic material is essential for an exact estimation of the machine's behaviour.

Keywords Electrical machines, Iron losses, Soft magnetic materials, Magnetoelasticity

Paper type Research paper

1. Introduction

The magnetic properties of non-grain-oriented electrical steels are prone to mechanical stresses, i.e. residual, external or thermal ones. In rotating electrical machines, mechanical stresses are ubiquitous and are of diverse origin, such as, e.g., material processing, machine construction and operation conditions.

As a result, the efficiency and specific losses of the machine are largely altered by the different states of mechanical stress. To improve rotating electrical machines in terms of energy efficiency and operational characteristics, the interdependence of mechanical stresses and magnetic properties variation needs to be studied. Within the past decades, many researchers have worked on the magnetoelastic coupling being closely related to magnetostriction (Jiles, 1995) and its consequences for the magnetic properties of electrical

This work is originated as part of the research training group GRK 1856 by the Deutsche Forschungsgesellschaft (DFG).

COMPEL - The international journal for computation and mathematics in electrical and electronic engineering
Vol. 36 No. 3, 2017
pp. 580-592

0332-1649
DOI 10.1108/COMPEL-09-2016-0416

steel sheets (Iordache and Hug, 2004; Feliziani *et al.*, 2008; Salinas-Beltrán *et al.*, 2016). The inverse magnetoelastic effect (Villari effect) describes the effect of mechanical stress on the magnetic properties (Bozorth, 1993).

In this study, the examined correlation of mechanical stress and strain with magnetic properties leads to a detailed magnetic characterisation of mechanically stressed soft magnetic material specimens which directly relate to actual characteristics of electrical steel laminations in electrical machines. Concurrent with developments concerning improved power density and performance of these applications, the focus is put to magnetic flux densities and high frequencies.

In electrical machines, the knowledge about the behaviour of specific iron losses dependent on the mechanical stress $p_{\mathrm{iron}}\ (B, f, \sigma)$ in the post-processing part of machine design is necessary. In Permiakov *et al.* (2004), the iron loss parameters for hysteresis, classical and excess loss components (Bertotti, 1988) dependent on compressive and tensile stresses are studied. As a conclusion, it is shown that the hysteresis and excess loss component behave similar when subject to a mechanical stress within the elastic region. In Singh *et al.* (2015), the influence of mechanical stress on the excess loss component is investigated. Studies in Saeed *et al.* (2015) result in a polynomial description of the stress-dependent hysteresis loss parameter with focus on mechanical compressive stresses.

This paper discusses the effect of applied tensile stress up to 100 MPa on the iron loss components, with the focus on high frequencies and magnetic flux densities. In contrast to Singh *et al.* (2015) and Saeed *et al.* (2015), a stress-dependent non-linear loss component is added to get a better prediction for high magnetic flux densities. Based on magnetic measurements of specimens consisting of electrical steel sheet loaded by different mechanical stress levels, the iron loss parameters for each loss component are identified. The measurements are performed in a standard single-sheet tester (SST). As a result, the stress-sensitivity of each loss parameter is identified and described.

2. Measurement

2.1 Experimental setup

Specimens of non-oriented electrical steel sheet are examined. Each studied sample has a length of l_{specimen} = 600 mm, a width of w_{specimen} = 100 mm and a thickness of d_{specimen} = 0.35 mm. Samples are oriented parallel to the rolling direction (RD) of the steel strip. Due to a low thickness of the studied material, tests with compressive forces lead to a buckling of the specimens (Euler's critical load). Therefore, only tensile forces are applied to the specimens.

An SST equipped with a hydraulic pressure cylinder can load specimens of electrical steel sheet with a maximum force of $F_{\mathrm{min,max}} = \pm 5$ kN homogeneously (Figure 1). Due to the geometrical conditions, i.e. widths and thickness of the studied samples, the maximum stress level is $\sigma_{\mathrm{min,max}} = \pm 142.9$ MPa. The force is transmitted onto the specimens via clamping jaws, where one side is fixed and the other side is moveable and controlled by the pressure cylinder. Stress and magnetic flux are applied collinearly (uni-axial loading).

The SST is incorporated into a computer-aided setup in accordance with the international standard (DIN IEC 60404–3:2010–05, 2010). The samples are characterised using controlled sinusoidal magnetic flux density with a form factor error of less than 1 per cent in the frequency range from quasi-static (100 mT/s) to 1 kHz.

2.2 Mechanical measurement

The changes in magnetic properties loaded by nominal stress within the elastic area of the material are studied. The elastic behaviour of the specimen is proofed by measuring the

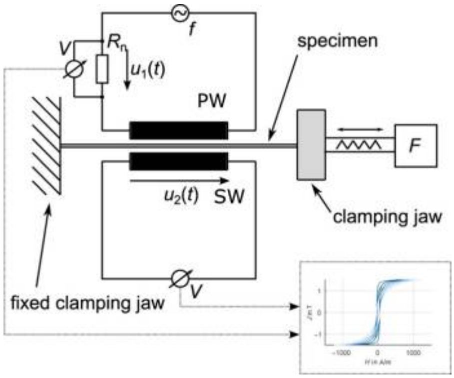

Figure 1.
Measuring principle (SST and hydraulic pressure cylinder)

Cauchy (engineering) strain of one sample while applying a mechanical nominal stress without a magnetic field. The Cauchy strain is measured by a half-bridge strain gauge adhered to the centre of one specimen. The measuring result depicts an elastic behaviour in the applied stress region with the determined mechanical properties in Table I.

3. Iron loss model

The semi-physical model for iron losses in Eggers *et al.* (2012) describes the iron loss behaviour for a wide range of frequencies. The model is based on Bertotti's model for iron losses (Bertotti, 1988). The description for iron losses is separated into a hysteresis, a classical (Foucault) eddy current and an excess loss component. Each component is motivated by a physical origin. An additional term considers the effect of the material non-linearity on the loss behaviour, i.e. due to saturation of the hysteresis curves, which gives a good estimation of the specific iron losses for high values of the magnetic flux density (Eggers *et al.*, 2012; Steentjes *et al.*, 2013).

Splitting the equation into a static and dynamic component, the specific iron loss description becomes:

$$p_{\mathrm{iron}} = p_{\mathrm{stat}} + p_{\mathrm{dyn}} \tag{1}$$

with

$$p_{\mathrm{stat}} = p_{\mathrm{hys}} = a_1 \cdot B^{\alpha} \cdot f \tag{2}$$

and

$$p_{\mathrm{dyn}} = p_{\mathrm{cl}} + p_{\mathrm{nl}} + p_{\mathrm{exc}} = a_2 \cdot B^2 \cdot f^2 + a_2 \cdot a_3 \cdot B^{2+a_4} \cdot f^2 + a_5 \cdot B^{1.5} \cdot f^{1.5} \tag{3}$$

where B is the peak value of the magnetic flux density and f its frequency.

Table I.
Mechanical properties of studied material

Description	Symbol	Value
Yield strength	σ_{y}	361 MPa
Young's modulus	E	210 GPa
Tensile strength	σ_{TS}	471 MPa

In contrast to Eggers *et al.* (2012), here, the hysteresis loss exponent α in equation (2) is extended to account for the fact that the full polarisation dependence of hysteresis cannot be described by a single power function representation (Leuning *et al.*, 2016; Chen and Pillay, 2002; Vandenbossche *et al.*, 2012):

$$\alpha = \alpha_0 + \alpha_1 \cdot B \tag{4}$$

The static or hysteresis component parameters a_1, α_0 and α_1 are determined by parameter fitting using the method of least squares to minimise the error between DC measurement results for the specific hysteresis energy and the static loss estimation.

The classic iron loss component considers the loss which occurs due to non-local eddy currents in the magnetic material. Using Maxwell's equations, the classical iron loss parameter a_2 is determined by Bertotti (1988) to:

$$a_2 = \frac{\pi^2 \cdot d^2}{6 \cdot \rho \cdot \rho_e} \tag{5}$$

where d is the thickness of the material, ρ the material density and ρ_e the specific electrical resistivity.

The excess loss component describes the additional eddy currents that occur around moving domain walls. For low frequencies, where the influence of the skin effect (Zirka *et al.*, 2010) and, additionally, the effect of non-linear loss component is insignificant, the excess loss component and its parameter can be calculated by:

$$p_{exc} = p_{meas} - p_{hys} - p_{cl} \tag{6}$$

where p_{meas} are the measured losses. In Eggers *et al.* (2012), it is suggested to use measurements with $f = 5$ Hz to extract the excess loss component.

To account for measured losses at higher magnetic flux densities ($B > 1$ T), a so-called non-linear or saturation loss component is added which considers the non-linear material behaviour for high frequencies and magnetic flux densities (Jacobs *et al.*, 2009). The non-linear loss parameters are estimated by mathematical parameter identification. Results in Eggers *et al.* (2012) show that these non-linear component lead to a good prediction of iron losses for high frequencies and high flux densities. Petrun *et al.* (2016) confirms the good agreement.

In Figure 2, the iron loss estimation for an unstressed specimen of the non-oriented steel sheet material M250-35A and various frequencies up to 1 kHz is shown. The estimation of the used iron loss parameters is explained in the following section. It can be seen that the iron loss prediction is a good approximation to the measurement with a relative small estimation error.

Tensile stresses cause a shear of the hysteresis curves. Measurements in Figure 3 show a shear in the hysteresis curves frequencies up to 1 kHz. The amount of magnetic field to reach designated polarisations at increasing tensile stresses is increasing. For all studied frequencies and maximum magnetic polarisations, the coercivity increases while the magnetic remanence decreases for a rise of mechanical tensile stress. The shear of the hysteresis curves is caused by a degradation of the domain structures and thus a change in the amount of required energy. Elastic deformations cause changes in the domain structure (Le Châtelier equilibrium principle) dependent on the induced magnetoelastic energy E_{me} (Cullity and Graham, 2009; Singh *et al.*, 2015). In this case, as a consequence, the iron losses which are dependent on the area of the hysteresis curve increase, characterising the material's sensitivity of magnetic properties to external mechanical stress.

In Figure 4, the static and dynamic stress-dependent loss components for two different operating points are shown [see equation (1)]. The dynamic loss component is determined by calculating the difference of measured total losses and static losses for each stress level. Seemingly, for small mechanical stresses up to approximately 20 MPa, the static loss proportion decreases and then starts to increase slightly. For higher frequencies, the same behaviour is observable. For f = 50 Hz, the dynamic loss component reaches its maximum proportion at approximately 20 MPa and then remains almost constant. For f = 1 kHz, an increase of the dynamic loss component is noticeable before reaching an upper limit for high stress values.

Due to the shear of the hysteresis curves and as a result of a variation in the magnetic parameters such as coercivity and magnetic remanence, the static loss component (2) is dependent on the mechanical stress:

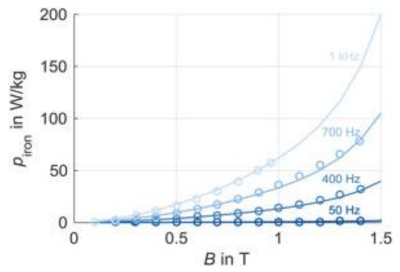

Figure 2. Calculated (—) and measured (◯) specific iron losses of unstressed specimens of M250-35A for different frequencies with $a_1 = 0.00816$, $a_2 = 3.66 \cdot 10^{-5}$, $a_3 = 0.15889$, $a_4 = 3.27680$, $a_5 = 0.0005$, $\alpha_0 = 1.19076$, $\alpha_1 = 0.79839$

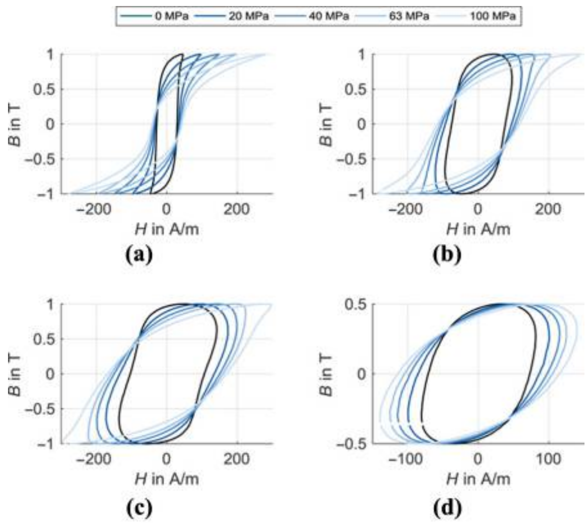

Notes: (a) f = 50 Hz, B_{max} = 1 T; (b) f = 400 Hz, B_{max} = 1.5 T; (c) f = 700 Hz, B_{max} = 1 T; (d) f = 1 kHz, J_{max} = 0.5 T

Figure 3. Measured stress-dependent hysteresis curves of M250-35A for different operating points

$$p_{\text{stat}}(B,f,\boldsymbol{\sigma}) = p_{\text{hys}}(B,f,\boldsymbol{\sigma}) = a_1(\boldsymbol{\sigma}) \cdot B^{\alpha_0(\sigma)+\alpha_1(\sigma)\cdot B} \cdot f \tag{7}$$

The sensitivity of the parameters is determined in Section 4. As the magnetic flux densities vary for different mechanical stress values at a constant magnetic field, the exponent for the magnetic flux density is dependent on the mechanical stress as well.

For the dynamic loss component, equation (3) becomes:

$$\begin{aligned} p_{\text{dyn}}(B,f,\boldsymbol{\sigma}) &= p_{\text{cl}}(B,f) + p_{\text{nl}}(B,f,\boldsymbol{\sigma}) + p_{\text{exc}}(B,f,\boldsymbol{\sigma}) \\ &= a_2 \cdot B^2 \cdot f^2 + a_2 \cdot a_3(\boldsymbol{\sigma}) \cdot B^{2+a_4(\sigma)} \cdot f^2 + a_5(\boldsymbol{\sigma}) \cdot B^{1.5} \cdot f^{1.5} \end{aligned} \tag{8}$$

The classical loss component parameter is assumed to be independent on the mechanical stress for loads below yield strength. The parameter is solely described by material properties (Permiakov *et al.*, 2004).

4. Results

4.1 Hysteresis loss component

For each stress level, the results of the DC measurements (100 mT/s using a fluxmeter) are used to determine the parameters a_1, α_0 and α_1 using the stress-dependent curves of the specific energy (Figure 5). Due to the shear of the hysteresis curves, the amount of required specific energy e is generally increased for higher values of mechanical stress, though small tensile stresses can pose an exception. In this case, the total area of the hysteresis loop is smaller when

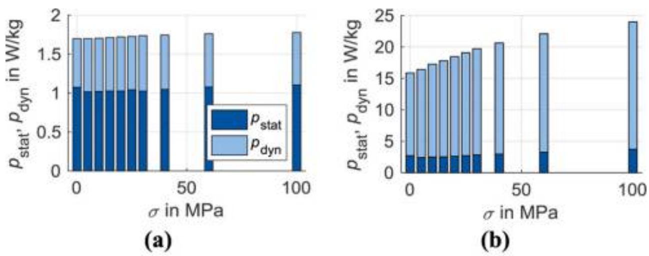

Notes: (a) f = 50 Hz, B = 1.5 T; (b) f = 1 kHz, B = 0.5 T

Figure 4. Static and dynamic loss components for two operating points

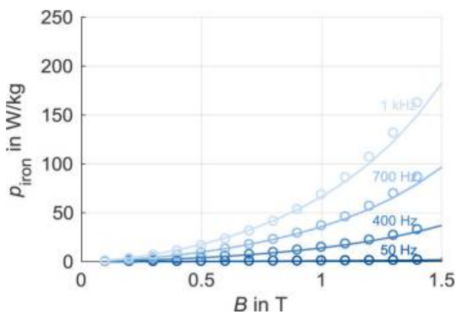

Figure 5. Stress-dependent specific energy e with calculated (–) and measured (○) data

compared to the unloaded state. Particularly for magnetic flux densities between 0.5 T and 1.5 T, a strong change of required energy between samples loaded differently can be observed.

Figure 6(a)-(c) depicts the trend of the hysteresis parameters a_1, α_0 and α_1 dependent on the mechanical stress level. It is apparent that for small stress values up to approximately 20 MPa, most of the variation of the parameters occurs. Due to a shear in the hysteresis curves for higher stress values and thus an increased demand of coercivity, parameter a_1 increases in the complete area. Parameter α_0 rises for small stress values before reaching its peak at approximately 25 MPa. Then, a slight decrease occurs. Parameter α_1 declines for the entire area. A similar behaviour is observed for the RD and the transverse direction for the elastic region (Leuning *et al.*, 2016).

4.2 Eddy current loss component

Table II collects the required data for the determination of the eddy current loss parameter [see equation (5)].

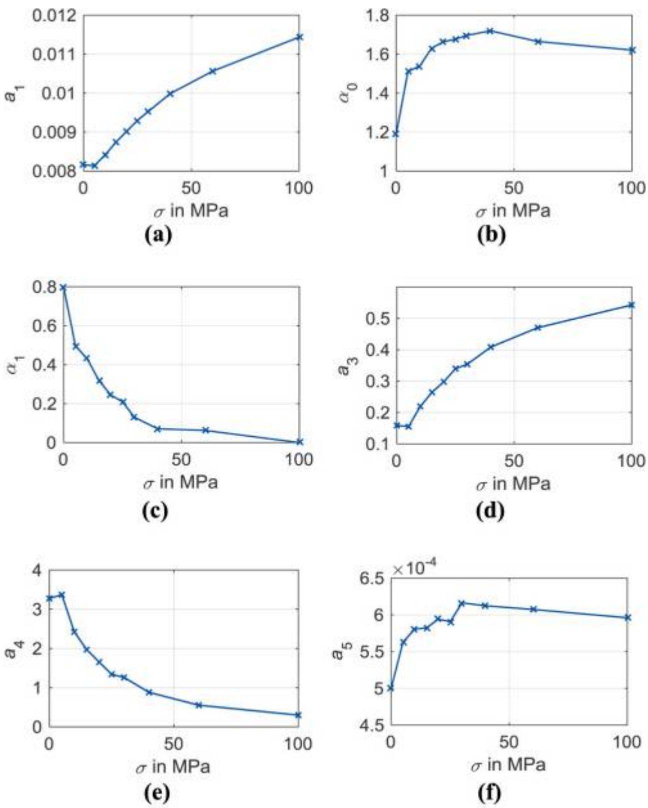

Notes: (a) Hysteresis loss parameter; (b) hysteresis loss exponent; (c) hysteresis loss exponent; (d) non-linear loss parameter; (e) non-linear loss exponent; (f) excess loss parameter

Figure 6.
Parameters' each loss component dependent on mechanical stress

The material density is according to the standard (DIN EN 10106:2016–03, 2016). The electrical resistivity is measured by four-terminal sensing, i.e. an uncoated square-cut sample of the same material with an edge length of 120 mm is fixed between a frame out of copper and connected to a DC current source. Setting a small current and measuring the voltage drop over the sample gives its resistance written in Table II. The eddy current loss parameter is then determined using equation (5) to $a_2 = 3.66 \cdot 10^{-5}$.

4.3 Excess loss component

Determining the excess loss parameter a_5, it is noticeable that the excess loss component first increases for around 30 MPa before the parameter starts to decrease slightly for higher mechanical stresses [Figure 6(f)]. The behaviour of the increasing trend of excess loss for small stresses can be explained by the deterioration of the domain walls.

4.4 Non-linear loss component

The parameters for the non-linear loss component are determined for each studied stress level by using mathematical parameter identification. The trend of a_3 first decreases before it begins to increase steeply. The behaviour of the non-linear loss coefficient shows a strong dependency on mechanical tensile stresses. It is suggested that due to the shear in the hysteresis curve while applying a tensile stress, the non-linear loss component has a significant influence. In contrast to parameter a_3, the parameter in the exponent a_4 becomes very small for high stress values after reaching a peak at 5 MPa [Figure 6(d) and (e)]. Consequently, the influence of the magnetic flux density on the non-linear losses is reduced for high stress values, whereas in the middle range of flux density, the influence of mechanical tensile stress is existent.

4.5 Total stress-dependent iron losses

Using equations (7) and (8), the total stress-dependent specific iron losses and its components are calculated for various operating points (Figure 7). The contribution of the different loss components on total iron losses varies depending on frequency. As for low frequencies, static hysteresis losses are dominant because they increase linearly with frequency [equation (7)], whereas the classical eddy current losses and non-linear losses exhibit a quadratic dependence on frequency [equation (8)] (Figure 8). For the hysteresis loss component, the most distinct stress-dependency can be seen for magnetic flux densities of $B = 1$ T, which is also validated by measurements (Figure 9). As described in Section 3, the non-linear or saturation loss component considers the non-linear material behaviour for high frequencies and magnetic flux densities, and its influence is therefore subordinate for low frequencies and polarisations. Accordingly, for increasing frequencies, it is apparent that the eddy current loss component expands and becomes the most dominant loss component for the frequency range of 400 Hz up to 1 kHz.

With increasing tensile stress, the hysteresis loss component shows a distinct progression. The frequency only affects the magnitude of the impact on total losses due to its linear dependency on frequency. For the operating point of 1.5 T at 50 Hz, it is

Name	Unit	Value
ρ	kg/m^3	7,650
ρ_e	μΩm	0.72
$d_{specimen}$	mm	0.35

Table II. Data to determine the classical loss component

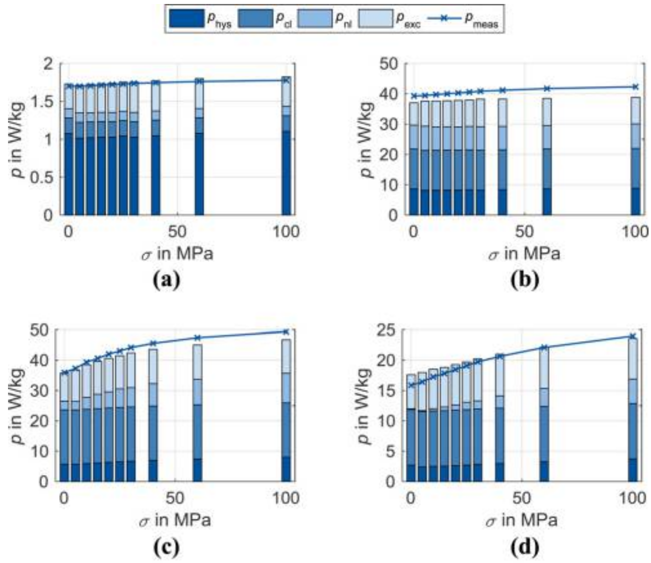

Figure 7. Proportion of loss components and comparison with measured losses for different operating points

Notes: (a) f = 50 Hz, B = 1.5 T; (b) f = 400 Hz, B = 1.5 T; (c) f = 700 Hz, B = 1 T; (d) f = 1 kHz, B = 0.5 T

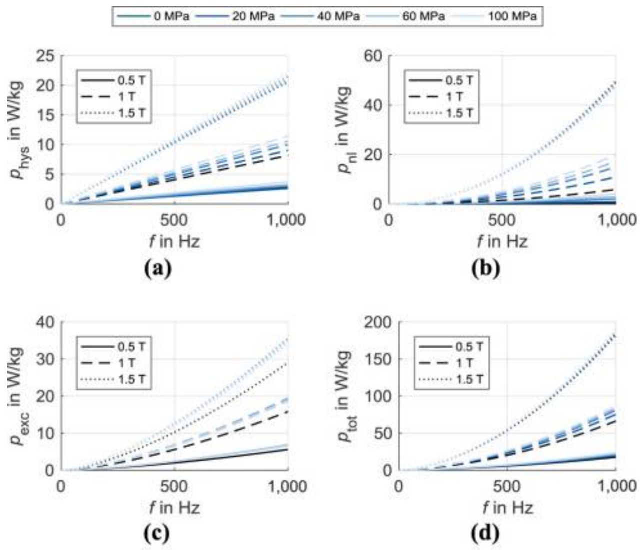

Figure 8. Modelled loss components and total losses for different magnetic flux densities dependent on the frequency for different mechanical stresses

Notes: (a) Hysteresis loss component; (b) non-linear loss component; (c) excess loss component; (d) total losses

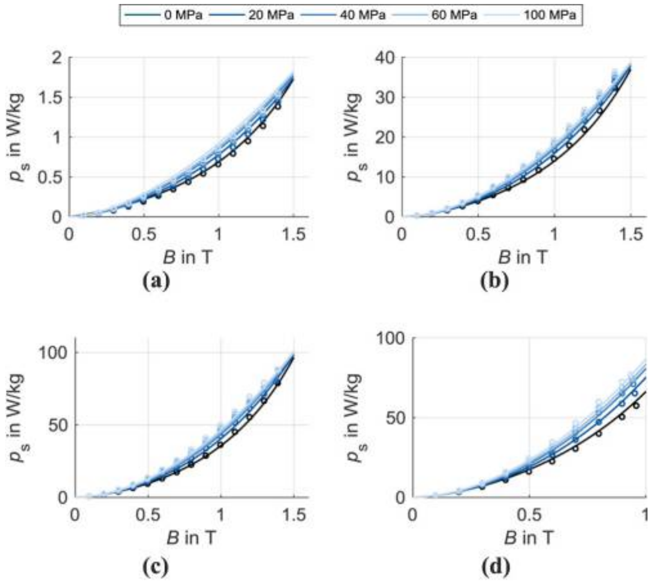

Notes: (a) f = 50 Hz; (b) f = 400 Hz; (c) f = 700 Hz; (d) f = 1 kHz

Figure 9. Calculated (–) and measured (○) iron losses dependent on magnetic flux densities and mechanical stress at different frequencies

observed that the impact of the further loss components is small and stays almost constant throughout all tensile loads. However, the dominance of hysteresis losses vanishes for higher frequencies and other loss components become dominant. The influence of tensile stress is considerable for higher frequencies affecting both excess and non-linear losses, although to a different extent. With increasing tensile stress, the excess loss component first starts to rise slightly and then remains almost constant for each examined frequency. As a conclusion, the influence of high mechanical stresses on excess losses is relatively small [Figure 8(c)]. The same result is described in Singh *et al.* (2015). In contrast to the hysteresis loss component, it is apparent that the influence of mechanical stress causes a significant variation in the non-linear and excess loss component for higher magnetic flux densities.

As result of this study, the non-linear loss component is sensitive to mechanical tensile stress for high frequencies [Figure 8(b)]. For low frequencies, the non-linear loss component is almost constant. For higher frequencies, the non-linear loss component becomes noticeable and increases for higher values of mechanical stress. Particularly for a flux density in the middle range (e.g. B = 0.5 T), the influence of stress on the non-linear loss component becomes significantly high. Regarding the hysteresis curves in Figure 2, the beginning of the saturation is shifted, i.e. the gradient of the B-H curve is lower than for the unstressed case. This causes the sensitivity of the non-linear loss component.

Due to the constant classical loss component, it is unaffected by mechanical stress. For high frequencies, it becomes the most dominant loss component.

Because the hysteresis loss component is only dominant for low frequencies, there is no minimum of total losses at small values of mechanical stress for higher frequencies. The highest sensitivity to mechanical stress is observable for the non-linear loss component for higher frequencies. The decreasing trend for the non-linear loss component while increasing the mechanical stress for high magnetic flux densities [Figure 8(b)] has to be analysed in an additional study.

For all plotted operating points, the stress-dependent iron loss prediction is a good approximation for the specific iron losses dependent on mechanical stress. Regarding Figure 10, it can be said that the absolute relative estimation error is smaller than 11 per cent. For 50 Hz and 1.5 T, the iron loss model overestimates the measured specific iron losses, while for 700 Hz and 1 T, the prediction underestimates the losses for the entire range of mechanical tensile stress. In contrast, the prediction for 1 kHz and 0.5 T produces the highest estimation error. The same behaviour can be observed in Figure 8, where a difference between measurement and prediction is apparent. Overall, the iron loss prediction gives a good description of the iron loss behaviour.

5. Conclusions

In this paper, the stress-sensitivity of the specific iron loss components is studied. The influence of mechanical stress on the iron losses is noticeable. The parameter study shows an increasing influence of the mechanical stress on the non-linear loss component, while the hysteresis loss component is dominant at low frequencies. The stress-dependent behaviour of the iron losses can be explained by the microstructural changes and its degradation of the domain structure inside the material. These effects cause a shear of the hysteresis curves and, as a consequence, a variation in the specific iron losses.

The stress-dependency is also sensitive to the frequencies and magnetic flux densities. Between 0.5 T and 1.5 T, the influence of mechanical stress causes a high variation in the iron losses. The results show that the variation in the hysteresis loss component becomes dominant for flux densities between 0.5 T and 1.5 T.

In contrast to Singh *et al.* (2015) and Saeed *et al.* (2015), the influence of high magnetic flux densities is modelled by an additional stress-dependent non-linear iron loss component, which considers iron losses originating from saturation. It is shown that the non-linear loss component is dependent on mechanical stress, while the excess loss component is mostly unaffected by high mechanical stresses.

The determined characteristics are valid for mechanical tensile stresses within the elastic region. The influence of mechanical stresses beyond the yield strength, meaning the plastic region, is the focus of continuing research as well as the study on the influence of compressive load on the magnetic properties and its induced variations in iron loss components. Studies using a wide range of different non-grain-oriented electrical steel sheet materials and different rolling directions are planned to verify the determined trends.

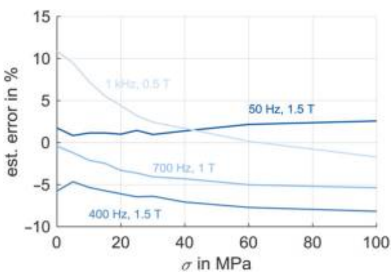

Figure 10.
Estimation error for predicted losses to measured losses for different operating points and dependent on mechanical stress

The results of this study can be used for a better prediction of the iron losses in electrical machines. Detailed investigations have to show the influence of mechanical stress induced, for example, due to shrink fitting or electromagnetic forces on the machine's behaviour and the efficiency.

References

Bertotti, G. (1988), "General properties of power losses in soft ferromagnetic materials", *IEEE Transactions on Magnetics*, Vol. 24 No. 1, pp. 621-630.

Bozorth, R.M. (1993), "Ferromagnetism", *An IEEE Press Classic Reissue*, IEEE Press, Wiley-Interscience, Piscataway, Hoboken, NJ.

Chen, Y. and Pillay, P. (2002), "An improved formula for lamination core loss calculations in machines operating with high frequency and high flux density excitation", *Conference Proceeding of Industry Applications Conference, Pittsburgh, 13-18 October, IEEE, Piscataway, NJ*, pp. 759-766.

Cullity, B.D. and Graham, C.D. (2009), *Introduction to Magnetic Materials*, 2nd ed., IEEE/Wiley, Hoboken, NJ.

DIN EN 10106:2016-03 (2016), "Cold rolled non-oriented electrical steel strip and sheet delivered in the fully processed state", EN 10106:2015.

DIN IEC 60404-3:2010-05 (2010), "Magnetic materials – Part 3: methods of measurement of the magnetic properties of electrical steel strip and sheet by means of a single sheet tester", IEC 60404-3:1992 + A1:2002 + A2:2009.

Eggers, D., Steentjes, S. and Hameyer, K. (2012), "Advanced iron-loss estimation for nonlinear material behavior", *IEEE Transactions on Magnetics*, Vol. 48 No. 11, pp. 3021-3024.

Feliziani, M., Belahcen, A. and Arkkio, A. (2008), "Locally coupled magneto-mechanical model of electrical steel", *COMPEL – The International Journal for Computation and Mathematics in Electrical and Electronic Engineering*, Vol. 27 No. 6, pp. 1451-1462.

Iordache, V.E. and Hug, E. (2004), "Effect of mechanical strain on the magnetic properties of electrical steels", *Journal of Optoelectronics and Advanced Materials*, Vol. 6 No. 4, pp. 1297-1303.

Jacobs, S., Hectors, D., Henrotte, F., Hafner, M., Gracia, M.H., Hameyer, K. and Goes, P. (2009), "Magnetic material optimization for hybrid vehicle PMSM drives", *World Electric Vehicle Journal*, Vol. 3, pp. 875-883.

Jiles, D.C. (1995), "Theory of the magnetomechanical effect", *Journal of Physics D: Applied Physics*, No. 28, pp. 1537-1546.

Leuning, N., Steentjes, S., Schulte, M., Bleck, W. and Hameyer, K. (2016), "Effect of elastic and plastic tensile mechanical loading on the magnetic properties of NGO electrical steel", *Journal of Magnetism and Magnetic Materials*, Vol. 417, pp. 42-48.

Permiakov, V., Dupré, L., Pulnikov, A. and Melkebeek, J. (2004), "Loss separation and parameters for hysteresis modelling under compressive and tensile stresses", *Journal of Magnetism and Magnetic Materials*, Vols 272/273/274/275/276.

Petrun, M., Steentjes, S., Hameyer, K. and Dolinar, D. (2016), "Comparison of static hysteresis models subject to arbitrary magnetization waveforms", in Belahcen, A., Demenko, A. and Pietrowski, W. (Eds), *Proceeding on the Conference of 24th Symposium on Electromagnetic Phenomena in Nonlinear Circuits (EPNC), Helsinki, 28 June-1 July, Aalto University, Helsinki*.

Saeed, O., Saleem, A., Rahman, T., Chromik, R. and Lowther, D.A. (2015), "Iron loss models under static stress for non-oriented and grain oriented steel", *Proceeding of 20th International Conference on the Computation of Electromagnetic Fields (Compumag), Montreal, 28 June-2 July, International COMPUMAG Society, Southampton*.

Salinas-Beltrán, J., Salinas-Rodríguez, A., Gutiérrez-Castañeda, E. and Deaquino Lara, R. (2016), "Effects of processing conditions on the final microstructure and magnetic properties in non-oriented electrical steels", *Journal of Magnetism and Magnetic Materials*, Vol. 406, pp. 159-165.

Singh, D., Rasilo, P., Martin, F., Belahcen, A. and Arkkio, A. (2015), "Effect of mechanical stress on excess loss of electrical steel sheets", *IEEE Transactions on Magnetics*, Vol. 51 No. 11, pp. 1-4.

Steentjes, S., Leßmann, M. and Hameyer, K. (2013), "Semi-physical parameter identification for an iron-loss formula allowing loss-separation", *Journal of Applied Physics*, Vol. 113 No. 17.

Vandenbossche, L., Jacobs, S., van Hoecke, D., Weber, B., Leunis, E. and Attrazic, E. (2012), "Improved iron loss modelling approach for advanced electrical steels operating at high frequencies and high inductions in automotive machines", *2nd International Electric Drives Production Conference (EDPC), IEEE*, Nuremberg, pp. 1-8.

Zirka, S.E., Moroz, Y.I., Marketos, P. and Moses, A.J. (2010), "Loss separation in nonoriented electrical steels", *IEEE Transactions on Magnetics*, Vol. 46 No. 2, pp. 286-289.

About the authors

Jan Karthaus received his MSc degree in Electrical Engineering from the RWTH Aachen University, Aachen, Germany, in September 2013. He has been working as a Research Associate at the Institute of Electrical Machines since November 2013. His research interests include iron loss computations, design and simulation of electrical machines, mechanical stress-dependency of ferromagnetic materials and electrical high-speed machines. Jan Karthaus is the corresponding author and can be contacted at: jan.karthaus@iem.rwth-aachen.de

Simon Steentjes received his Diploma degree in Electrical Engineering from RWTH Aachen University, Germany, in November 2011. He has been working as a Research Associate at the Institute of Electrical Machines since December 2011. His research interests include hard- and soft magnetic material modelling on the micro- and macroscopic scale, iron loss calculation, effects of material processing, magnetic forces and mathematical methods.

Nora Leuning is a Research Associate at the Institute of Electrical Machines at RWTH Aachen University. In July 2015, she graduated with an MSc degree in Materials Engineering. Her main research interests include studies of structural parameters and their resulting effect on magnetic behaviour of FeSi electrical steel during production and processing, modelling of material behaviour and incorporating effects of magnetic texture and anisotropy of NGOs.

Dr Kay Hameyer received his Diploma degree in Electrical Engineering from the University of Hannover and his PhD degree from the Berlin University of Technology, Germany. After his university studies, he worked with the Robert Bosch GmbH in Stuttgart, Germany, as a Design Engineer for permanent magnet servo motors and vehicle board net components. Until 2004, Dr Hameyer was a Full Professor for Numerical Field Computations and Electrical Machines with the KU Leuven in Belgium. Since 2004, he is a Full Professor and the Director of the Institute of Electrical Machines (IEM) at the RWTH Aachen University in Germany. He was the vice dean (in 2006) of the faculty and the dean (from 2007 to 2009) of the Faculty of Electrical Engineering and Information Technology of RWTH Aachen University. His research interests are numerical field computation and optimisation, the design and controls of electrical machines, in particular permanent magnet excited machines, induction machines and the design using the methodology of virtual reality. Since several years, Dr Hameyer's work is concerned with the magnetic levitation for drive systems, magnetically excited audible noise in electrical machines and the characterisation of ferro-magnetic materials. Dr Hameyer is the author of more than 250 journal publications, more than 500 international conference publications and four books. Dr Hameyer is a member of VDE, IEEE senior member and fellow of the IET.